Polarization active Raman spectroscopy and coherent Raman ellipsometry

S. A. Akhmanov, A. F. Bunkin, S. G. Ivanov, and N. I. Koroteev

Moscow State University
(Submitted 15 September 1977)
Zh. Eksp. Teor. Fiz. **74**, 1272–1294 (April 1978)

A new system of nonlinear laser spectroscopy is described, namely polarization active Raman spectroscopy (ARS) of light. The method is based on the study of the dispersion of the polarization characteristics of the anti-Stokes (or Stokes) signal on going through resonance. Measurement of the dispersion of the polarization rather than the intensity dispersion usually investigated in ARS (amplitude ARS), or the use of the polarization dispersion in amplitude ARS, extends the capabilities of active spectrocopy in some respects. First, measurement of the dispersion of the ellipticity of the polarization of the scattered radiation makes possible independent measurements of the dispersions of the real and imaginary parts of the susceptibility, with a relative accuracy $\sim 10^{-3}$–10^{-4} not attainable with amplitude spectroscopy. Second, the technique of resolving inhomogeneously broadened Raman bands is substantially improved; it becomes possible, to resolve lines separated by distances shorter than the homogeneous width in a large class of resonances. Finally, polarization ARS offers a new approach to measurement of the invariants of the scattering tensor; a comparison of the ARS data with spontaneous-scattering spectroscopy data makes it possible to separate distinctly the asymmetric part of the tensor. The theory of polarization ARS is developed; its new possibilities are demonstrated experimentally. In particular, the use of polarization effects makes it possible to suppress substantially the contribution of the nonresonant interactions that interfere with the registration of the Raman lines. The possibility of resolving the inner structure of inhomogeneously broadened lines is demonstrated with the HNO_3 spectrum as an example. The spectrum fine structure due to superposition of lines of different symmetry is revealed for the first time. Additional proof is obtained of the presence of considerable asymmetrical components of the Raman tensors of a number of depolarized lines in C_6H_6 and CCl_4.

PACS numbers: 42.65.Cq, 07.60.Fs

1. INTRODUCTION

1.1. Active Raman spectroscopy of light (ARS) has recently become (see the reviews[1-4] and the Conference Proceedings[5]) one of the most universal methods of nonlinear spectroscopy used for the investigation of gases, liquids, and solids. The physical idea of the method is the phasing of the elementary excitations (molecule vibrations or rotations in the case of Raman scattering (RS)) with the aid of biharmonic pumping by tunable lasers; the frequency difference $\omega_1 - \omega_2$ is scanned near the frequency Ω of the investigated resonance. Coherent molecular oscillations are probed with optical radiation of frequency ω (in many cases it is convenient to use $\omega = \omega_1$); the information on the medium is carried by a Stokes or anti-Stokes signal at the frequency[1)]

$$\omega_{S,a} = \omega \mp (\omega_1 - \omega_2).$$

The onset of radiation at the frequencies $\omega_{S,a}$ can be phenomenologically described as a four-photon process mediated by cubic nonlinearity with susceptibility $\chi^{(3)}$. From this point of view the task of the ARS is to study resonances in $\chi^{(3)}_{ijkl}$. Near the investigated resonance, it is convenient to write

$$\chi^{(3)}_{ijkl} = \mathrm{Re}\,\chi^{(3)}_{ijkl} + i\,\mathrm{Im}\,\chi^{(3)}_{ijkl} = \chi^{(3)NR}_{ijkl} + \chi^{(3)R}_{ijkl},$$

where $\chi^{(3)NR}$ is the "nonresonant" part of the susceptibility (it is connected with electronic, vibrational and rotational transitions that are far from ω_1 or ω_2 and their combinations), and $\chi^{(3)R}$ is the resonant part. For a solitary Raman resonance we have

$$\chi^{(3)R} = \tilde{\chi}^{(3)R} \frac{2\Omega\Gamma}{\Omega^2 - 2i\Gamma(\omega_1 - \omega_2) - (\omega_1 - \omega_2)^2}.$$

1.2. The simplest (and presently most widely used) variant of ARS is the socalled *amplitude* ARS and deals with the study of the dispersion of the intensity of the Stokes or anti-Stokes signal $I_{c,a} = I_{c,a}(\Delta)$, where $\Delta = [(\omega_1 - \omega_2) - \Omega]/\Gamma$. This method was used in a large number of studies (see, e.g.,[7-10]); it is particularly effective for strong RS lines, for which

$$\alpha = \tilde{\chi}^{(3)R}/\chi^{(3)NR} \gg 1.$$

This situation obtains, in particular, for cryogenic liquids and for strong transitions in gases. Amplitude ARS is effectively used in this case for high-resolution spectroscopy[11,12] and for an exact determination of the natural frequencies.[13] The amplitude ARS methods were used also for the first studies of double resonances, namely electron-vibrational,[14-18] vibrational-vibrational,[19] and exciton-vibrational.[20]

1.3. At the same time, recent studies have revealed also that the method of amplitude ARS is subject to some limitations. Appreciable difficulties arise in the study of lines with $\alpha \leqslant 1$ and of inhomogeneously broadened bands.[2] Therefore in many problems connected with the investigation of condensed media, amplitude ARS turned out to be less effective than spontaneous Raman scattering (SpRS) spectroscopy. It must also be emphasized that in the usual variant of amplitude ARS the information on the medium is incomplete. Thus, in the overwhelming majority of work on the isotropic media what was actually measured was the dispersion

 0038-5646/78/040667-12$02.40

of the component $\chi^{(3)}_{1111}$ of the cubic-susceptibility tensor. Attempts to overcome the shortcomings of amplitude ARS are dealt with in many recent papers. These include work on phase ARS,[22] on the optical Kerr effect induced by Raman resonance,[23] on spectroscopy that makes use of the Raman enhancement effect.[24] The most promising and universal method, however, is in our opinion polarization ARS based on the study of the polarization characteristics of an anti-Stokes (or Stokes) signal as it goes through resonance. The present paper is devoted to an exposition of the results of a theoretical and experimental study of this method.

1.4. The polarization measurements in SpRS spectra yield, as is well known, extensive information on the medium.[25-27] In ARS, which operates with the fourth-rank tensor $\chi^{(3)}_{ijkl}$, these possibilities are naturally greater; this has already been pointed out.[7,8] This, however, is not all; just as in other types of nonlinear spectroscopy (see, e.g.,[28] where saturation polarization spectroscopy is described), the use of polarization measurements makes for a much better resolution and accuracy, and in ARS these possibilities are particularly extensive. At our laboratory we developed two variants of polarization ARS.

A. The first, which can be called polarization-amplitude ARS, is based on the difference between the polarization of the nonlinear sources that are connected with $\chi^{(3)NR}$ and $\chi^{(3)R}$. As a result, amplitude ARS without a coherent background is possible. The use of this circumstance has made it possible[29-31] to add substantially to the capabilities of the ARS of weak lines and of gas analysis with the aid of ARS. This procedure is closely related to a method described in[23], but is more effective in many respects. A more complicated variant of polarization–amplitude ARS is described in[32].

B. Another method, in which one registers directly the dispersion of the polarization of the scattered signal, can be called coherent Raman ellipsometry.[33]

1.5. The present article contains an exposition of new data on polarization ARS and is a further development of[30,33]. Principal attention is paid to increasing the accuracy of the measurement of the nonlinear-susceptibility dispersion, to resolution of the structure of the inhomogeneously broadened RS bands, and to the determination of the conditions under which maximum possible information on the scattering tensor can be obtained by ARS methods.

In Sec. 2 we consider polarization effects in amplitude ARS. The most interesting among them, besides the already mentioned suppression of the coherent background, are the singularities of the manifestation in the ARS of the isotropic (scalar), anisotropic (quadrupole), and antisymmetric (magnetic-dipole) parts of the RS tensor, and also the unique possibility of shaping the Raman-resonance contour by varying the polarization conditions. The latter circumstance, together with the interference, typical of ARS, between closely lying resonances, can be effectively utilized to resolve inhomogeneously broadened structureless bands in the spontaneous RS spectra produced by superimposed lines of different symmetry.

In Sec. 3 are present the principles of coherent RS ellipsometry and the experimental results obtained with its aid. The main advantage of this variant of polarization ARS is the high accuracy of the data it yields on the dispersion of $\chi^{(3)}(\omega_a; \omega_1, \omega_1, -\omega_2)$, since the fluctuations of the pump-wave intensity do not spill over to the fluctuations of the polarization of the anti-Stokes signal, while the fluctuations of the pump-laser beam polarizations are as a rule small.

Another important advantage of coherent ellipsometry is the possibility it affords of simultaneously and independently measuring the dispersions of the real and imaginary parts of the susceptibility $\chi^{(3)}(\omega_a; \omega_1, \omega_1, -\omega_2)$. At the same time, in polarization spectra, as well as in the amplitude "active" spectra, it becomes possible to observe interference of various superimposed lines and to study their fine structure.

In Sec. 4 are given experimental results in which the inhomogeneously broadened band of concentrated nitric acid was resolved, for the first time ever, by the method of polarization ARS. The interference of the different components within the inhomogeneously broadened band is clearly revealed.

1.6. In the Conclusion it is emphasized that although the method of coherent ellipsometry has been developed for Raman spectroscopy, it can be readily generalized to measurements of the dispersion of cubic susceptibility near resonances of other types. This circumstance may be of special interest also for nonlinear spectroscopy of crystals.

2. POLARIZATION EFFECTS IN AMPLITUDE ARS

2.1. *Polarization of nonlinear source.* In an isotropic medium, three components of the nonlinear-susceptibility tensor are independent. For the ARS scheme with anti-Stokes signal at the frequency $\omega_a = 2\omega_1 - \omega_2$, the number of independent components decreases to two. We shall therefore deal henceforth with three components of the susceptibility I, connected by the relation

$$\chi^{(3)}_{1111}(\omega_a; \omega_1, \omega_1, -\omega_2) = 2\chi^{(3)}_{1122}(\omega_a; \omega_1, \omega_1, -\omega_2) + \chi^{(3)}_{1221}(\omega_a; \omega_1, \omega_1, -\omega_2).$$

For the polarization vector of a nonlinear source we obtain in this case, using formulas (A.4) and (A.6)–(A.10) of the Appendix

$$\frac{\mathbf{P}^{(3)}(\omega_a)}{(E^{(1)})^2 E^{(2)*}} = \frac{\mathbf{P}^{(3)NR}(\omega_a) + \mathbf{P}^{(3)NR}(\omega_a)}{(E^{(1)})^2 E^{(2)*}} = \chi^{(3)NR}_{1111}(\omega_a; \omega_1, \omega_1, -\omega_2)\mathbf{P}_{NR} + \chi^{(3)R}_{1111}(\omega_a; \omega_1, \omega_1, -\omega_2)\mathbf{P}_R, \quad (1)$$

where[3)]

$$\mathbf{P}_{NR} = 2\mathbf{e}_1(\mathbf{e}_1\mathbf{e}_2^*) + \mathbf{e}_2^*(\mathbf{e}_1\mathbf{e}_1), \quad (2)$$

$$\mathbf{P}_R = 3(1-\rho)\mathbf{e}_1(\mathbf{e}_1\mathbf{e}_2^*) + 3\rho\mathbf{e}_2^*(\mathbf{e}_1\mathbf{e}_1); \quad (3)$$

$\mathbf{e}_1$ and $\mathbf{e}_2$ are the unit vectors of the generally complex polarizations of the pump waves:

$$\mathbf{E}^{(1,2)} = \mathbf{e}_{1,2}E^{(1,2)}, \quad |\mathbf{e}_{1,2}| = 1;$$

and finally

$$\bar{\rho}=(1/15g^2-1/6g_a^2)/(b^2+1/15g^2)=\chi^{(3)R}_{1221}/\chi^{(3)R}_{1111}. \quad (4)$$

In the case when $g_a=0$ (the RS tensor is symmetric), we have $\bar{\rho}=\rho$, where ρ is the degree of depolarization of the spontaneous RS line. In the opposite case $\bar{\rho}=(\mathcal{P}-\rho)/(1+\mathcal{P})$, where $\mathcal{P}$ is the coefficient of the reversal of the RS line in the case of forward scattering.[25-27]

On the other hand, using relations (A.8)-(A.10) of the Appendix, we can resolve the resonant component of the nonlinear source (1) into parts corresponding to isotropic, antisymmetrical and anisotropic scattering:

$$\frac{\mathbf{P}^{(3)R}(\omega_a)}{(E^{(1)})^2E^{(2)*}}=\chi_0\mathbf{P}^{(3)R}_{is}+\chi_1\mathbf{P}^{(3)R}_{ant}+\chi_2\mathbf{P}^{(3)R}_{anis}, \quad (5)$$

$$\chi_0=b^2\frac{NL^4}{24M\Omega\Gamma}(-i-\Delta)^{-1},\quad \mathbf{P}^{(3)R}_{is}=3\mathbf{e}_1(\mathbf{e}_1\mathbf{e}_2^*), \quad (6)$$

$$\chi_1=\frac{1}{2}g^2\frac{NL^4}{24M\Omega\Gamma}(-i-\Delta)^{-1},\quad \mathbf{P}^{(3)R}_{ant}=\mathbf{e}_1(\mathbf{e}_1\mathbf{e}_2^*)-\mathbf{e}_2^*(\mathbf{e}_1\mathbf{e}_1), \quad (7)$$

$$\chi_2=\frac{4}{45}g^2\frac{NL^4}{24M\Omega\Gamma}(-i-\Delta)^{-1},\quad \mathbf{P}^{(3)R}_{anis}=\frac{3}{4}\mathbf{e}_1(\mathbf{e}_1\mathbf{e}_2^*)+\frac{9}{4}\mathbf{e}_2^*(\mathbf{e}_1\mathbf{e}_1). \quad (8)$$

A representation similar to (5) is obtained also as a result of direct expansion of the quantum-mechanical expression for the tensor $\chi^{(3)R}_{ijkl}$ into irreducible tensor sets.[34]4)

It is seen from (1)-(3) that when circularly polarized pump waves are used a nonzero anti-Stokes signal is obtained only when the polarization vectors in the two waves rotate at frequencies ω_1 and ω_2 in the same direction (the rotation in the wave of the anti-Stokes component is also in the same direction).

When linearly polarized pump waves are used, the anti-Stokes signal differs from zero when their polarizations are varied in a wide range. Figure 1 shows for this case the relative positions of the polarization unit vectors of the pump waves and of the different components $\mathbf{P}^{(3)R}_{ant}$ and $\mathbf{P}^{(3)R}_{anis}$ of the resonant part of the nonlinear source at the frequency ω_a. The figure shows also the orientation $\mathbf{P}_{NR}$ of the nonresonant part of this source and the geometric loci of the ends of these vectors when the angle φ between the polarization unit vectors $\mathbf{e}_1$ and $\mathbf{e}_2$ is varied.

2.2. *Elimination of nondispersing pedestal from spectra obtained in ARS.* As seen from (2) and (3) and Fig. 1b, the polarization vectors of the resonant ($\mathbf{P}_R$) and nonresonant ($\mathbf{P}_{NR}$) components of the nonlinear source $\mathbf{P}^{(3)}(\omega_a)$ are inclined to each other by a certain angle θ that differs from zero at $\bar{\rho}\neq 1/3$:

$$\operatorname{tg}\theta=(3\bar{\rho}-1)\operatorname{tg}\varphi/(3+\bar{\rho}\operatorname{tg}^2\varphi). \quad (9)$$

This circumstance makes possible discrimination of the "coherent background" generated by $\mathbf{P}_{NR}$. To this end it is necessary to place in the path of the anti-Stokes wave a specially oriented polarization analyzer.[30] Let $\mathbf{P}_\epsilon$ be a unit vector that specifies the plane of oscillations that pass through the analyzer (it makes an angle ϵ with the normal to the vector $\mathbf{P}_{NR}$ (see Fig. 1b). Then the projection of the polarization vector of the nonlinear

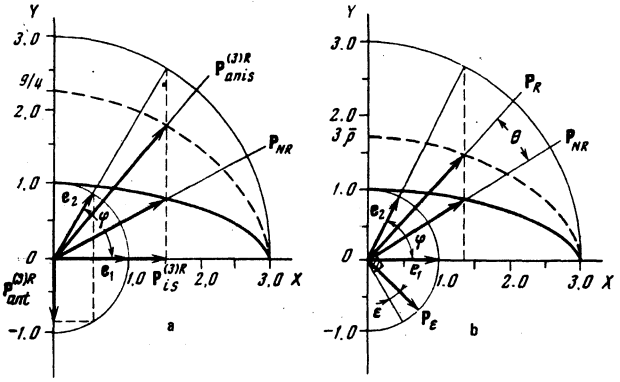

FIG. 1. Relative arrangement of the polarization unit vectors $\mathbf{e}_1$ and $\mathbf{e}_2$ of the pump wave and of the various components of the polarization vector $\mathbf{P}^{(3)}(\omega_a)$ of the nonlinear source. a) The components $\mathbf{P}^{(3)R}_{is}$, $\mathbf{P}^{(3)R}_{ant}$, and $\mathbf{P}^{(3)R}_{anis}$, corresponding respectively to the isotropic, antisymmetrical, and anisotropic scattering; the geometric locus of the end points of these vectors, when the angle φ between $\mathbf{e}_1$ and $\mathbf{e}_2$ is varied, is a straight line parallel to $\mathbf{e}_1$ for $\mathbf{P}^{(3)R}_{is}$, a straight line perpendicular to $\mathbf{e}_1$ for $\mathbf{P}^{(3)R}_{ant}$, and an ellipse with semiaxes 3 and 9/4 for $\mathbf{P}^{(3)R}_{anis}$. b) The vectors $\mathbf{P}_R$ and $\mathbf{P}_{NR}$ corresponding to the resonant Raman and the nonresonant electronic contributions to the nonlinear source. The geometric locus of these vectors, when φ is varied, is an ellipse with semiaxes 3 and 1 for $\mathbf{P}_{NR}$ and an ellipse with semiaxes 3 and $3\bar{\rho}$ for $\mathbf{P}_R$; $\mathbf{P}_\epsilon$ is a unit vector that specifies the plane of the oscillations passed by the analyzer, with ϵ reckoned from the normal to $\mathbf{P}_{NR}$.

source (1) on the plane of the oscillations that pass through the analyzer is given by

$$\frac{\mathbf{P}^{(3)}(\omega_a)\mathbf{P}_\epsilon}{(E^{(1)})^2E^{(2)*}}=\lambda_\epsilon=\chi^{(3)NR}_{1111}(8\cos^2\varphi+1)^{1/2}\sin\epsilon$$

$$+\frac{3\chi^{(3)R}_{1111}}{2(8\cos^2\varphi+1)^{1/2}}\{(1-3\bar{\rho})\cos\epsilon\sin 2\varphi+2[3-(3-\bar{\rho})\sin^2\varphi]\sin\epsilon\}. \quad (10)$$

We see that the analyzer can be so mounted ($\epsilon=0$) that the anti-Stokes component passed by the analyzer will contain no component generated by the non-resonant component $\mathbf{P}_{NR}$ of the linear source; in this case

$$\frac{\mathbf{P}^{(3)}(\omega_a)\mathbf{P}_{\epsilon=0}}{(E^{(1)})^2E^{(2)*}}=\frac{3\sin 2\varphi}{(8\cos^2\varphi+1)^{1/2}}(\chi^{(3)R}_{1122}-\chi^{(3)R}_{1221}). \quad (11)$$

Complete elimination of the coherent background in the ARS spectra is prevented by processes that lead to depolarization of the pump waves and of the coherently scattered radiation.

2.3. *Control of the relative signs of the resonant and nonresonant contributions to the nonlinear source and formation of the contour of the signal dispersion curve in polarization ARS.* The frequency dependence of the intensity of the anti-Stokes signal $I_a(\omega_1-\omega_2)$ in the amplitude ARS near a solitary Raman resonance (see formula (7) of [8]) is determined by the relation

$$I_a(\omega_1-\omega_2)\propto|\lambda(\omega_1-\omega_2)|^2I_1^2I_2, \quad (12)$$

where

$$\lambda(\omega_1-\omega_2)=\mathbf{e}_a\cdot\mathbf{P}^{(3)}(\omega_a)/(E^{(1)})^2E^{(2)*}=\lambda_R(-i-\Delta)^{-1}+\lambda_{NR} \quad (13)$$

is the coefficient of the nonlinear coupling of the four-wave interaction;

$$\omega_a=2\omega_1-\omega_2,\quad \lambda_{R,NR}=(e_a^*)_i\chi_{ijkl}^{(3)R,NR}(e_1)_j(e_1)_k(e_2^*)_l;$$

$\mathbf{e}_a$ is a unit vector of the polarization of the anti-Stokes component field; I_1 and I_2 are the intensities of the pump waves. If, as assumed in Sec. 2.2, the anti-Stokes signal is registered after the passage through the polarization specified by the vector $\mathbf{P}_\epsilon$, then $\mathbf{e}_a$ must be identified with $\mathbf{P}_\epsilon$, so that when the dispersion curve (12) is calculated we can use expression (10), with

$$\lambda_{R,\epsilon}=\frac{3\chi_{1111}^{(3)R}}{2(8\cos^2\varphi+1)^{1/2}}\{(1-3\rho)\sin 2\varphi\cos\varepsilon+2[3-(3-\rho)\sin^2\varphi]\sin\varepsilon\},$$

$$\lambda_{NR,\epsilon}=\chi_{1111}^{(3)NR}(8\cos^2\varphi+1)^{1/2}\sin\varepsilon.$$

The shape of the dispersion curve (12) is the result of interference between the resonant (λ_R) and nonresonant (λ_{NR}) components of the nonlinear-coupling coefficient (13), and is determined by their relative values and sign. Since they depend on ϵ, it is clear that by varying the analyzer rotation angle ϵ we can effectively control the shape of the dispersion curve $I_a(\omega_1-\omega_2)$. In particular, if ϵ is varied in the range

$$0<\varepsilon<\theta \text{ at } \theta>0, \tag{14a}$$

or

$$\theta<\varepsilon<0 \text{ at } \theta<0 \tag{14b}$$

(θ is defined in (9)) the sign of the ratio $\lambda_{R,\epsilon}/\lambda_{NR,\epsilon}$ is the reverse of the sign of the same ratio when ϵ lies outside the indicated interval. This circumstance manifests itself in the spectrum in the fact that the minima in the plots of the intensity of the anti-Stokes signal against the frequency detuning $\omega_1-\omega_2$ lie in this case on opposite sides of the maximum. The geometrical interpretation of (14) follows from Fig. 1; (14) corresponds to the case when the projections of the vectors $\mathbf{P}_R$ and $\mathbf{P}_{NR}$ on the analyzer transmission plane (the vector $\mathbf{P}_\epsilon$) have opposite signs.

If we assume that the investigated medium has two Raman resonances characterized by the noncollinear vectors $\mathbf{P}_{R1}$ and $\mathbf{P}_{R2}$, then it is clear that by placing the analyzer in such a way that the projections of $\mathbf{P}_{R1}$ and $\mathbf{P}_{R2}$ on the vector $\mathbf{P}_\epsilon$ have opposite signs it is possible to alter radically the character of the mutual interference of these resonances in the active spectrum compared with the usual amplitude ASR scheme. In particular, in the case of closely located Raman resonances making resonant contributions of opposite sign to $\lambda(\omega_1-\omega_2)$, one can expect superposition of the minima and a substantial improvement of the conditions for the resolution of close lines.[35] This possibility will be discussed in detail in Sec. 4.

In Fig. 2, using as an example the toluene RS line with frequency $\Omega/2\pi c=1209$ cm^{-1}, we demonstrate the possibility of shaping the contour of an "active" spectrum by varying the polarization conditions. The transfer of the intensity minimum from the region of positive frequency detunings from the center of the Raman resonance ($\Delta>0$) into the region $\Delta<0$ takes place when the polarization analyzer is rotated several degrees near the position corresponding to complete cancellation of the coherent pedestal.

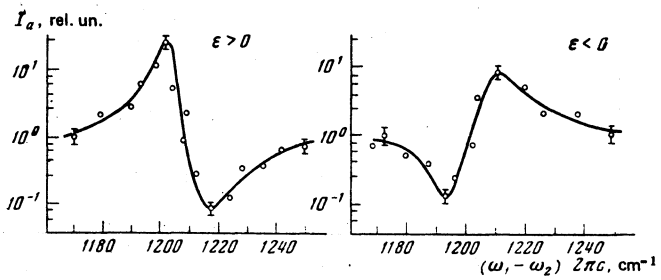

FIG. 2. Shaping of the contour of the Raman resonance curve of toluene by varying the polarization conditions; left—angle between the transmission plane of the analyzer and the normal to $\mathbf{P}_{NR}$ is $\epsilon\approx 2°$; right—angle $\epsilon=-3°$.

2.4. *Polarization ARS spectrometer.* The experimental setup used in our experiments on polarization ARS is shown in Fig. 3. The driving laser L (aluminum-yttrium garnet) was Q-switched and was operated repeatedly (12.5 Hz). Its 1.06-μm radiation was transformed, after passing through the amplifier, into the second harmonic ($\lambda=0.53$ μm) by a lithium-niobate crystal (SHG-1). A selective mirror directed that fraction of the master laser which was not converted into the second harmonic to a second frequency doubler SHG-2. This radiation ($\lambda_1=0.53$ μm) served as one of the pump wave with fixed frequency ω_1. The second pump wave (ω_2) came from a tunable laser (rhodamine-6Zh dissolved in ethanol) with continuous flow of the solution (lasing line width 0.5 – 2.5 cm^{-1}). The pump beams were focused into a cell C with the investigated substance. The radiation emerging from the cell was

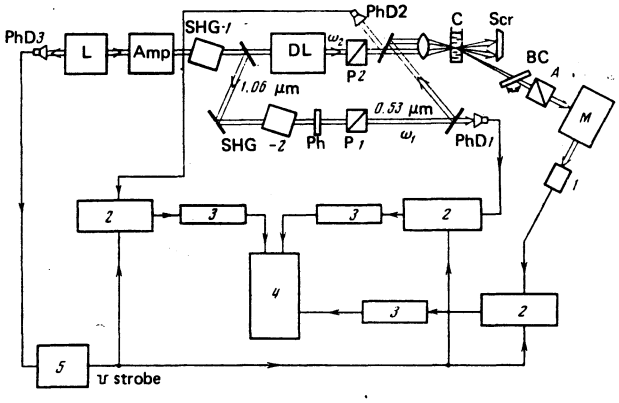

FIG. 3. Block diagram of experimental setup: L and Amp—YAG:Nd^{3+} laser and amplifier; SHG-1, SHG-2—frequency doublers using $LiNbO_3$ crystals: DL—dye laser (solution of rhodamine-6Zh in ethanol); P1, P2—Frank-Ritter polarization prisms; C—cell with investigated substance; Scr—screen blocking the direct pump rays; BC—rotating calcite Berek compensator; A—polarization analyzer; M—DFS-12 spectrometer; 1—FEU-79 photomultiplier; PhD1—PhD3—photodiodes; 2—strobed amplitude-digital converters (ADC); 3—transcriptors; 4—digital printout unit (DPU); 5—strobing-pulse generator synchronized with the master-laser pulse.

fed to a DFS-12 spectrograph that served as a monochromator. In the investigation of liquids, the collimation of the ARS signal and the satisfaction of the conditions of noncollinear synchronous wave interaction made it possible to get rid of most stray illumination due to the pump waves, using a diaphragm placed past the cell.[8] When gases were investigated, we used in addition interference filters. The angle φ between two planes of polarizations of the pump waves was set with the aid of two Frank-Ritter polarization prisms (P1-P2). The analyzer was either a Glan prism or a film polaroid.

The signal from the spectrograph output was registered with a photomultiplier, the pulsed signal from which was fed to a registration system consisting of a strobed bock of an amplitude-digital converter, a strobing-pulse generator, and a Ch3-34 electronic frequency meter. After accumulation in the frequency-meter memory for 12–13 or 125 laser flashes, the information was automatically recorded in digital form by a digital printout unit (DPU). To increase the accuracy with which the amplitude ARS spectra were measured in the registration system we used besides the main channel, two additional channels to control intensities I_1 and I_2 of the pump waves (PhD1 and PhD2). The DPU printed the data from all three channels. The measurement results were normalized with account taken of the dependence of the anti-Stokes signal intensity I_a on the intensities I_1 and I_2:

$$I_a(\omega_1-\omega_2)\propto|\lambda(\omega_1-\omega_2)|^2 I_1^2 I_2.$$

2. *Amplitude ARS: Experimental results and their discussion.* The experiments performed by us in a large number of liquids and in gas mixtures show that the increase of the contrast of the active spectra on account of the suppression of the non-dispersing pedestal by a polarization procedure is many cases quite effective (see[29-31]). In all the organic solvents investigated by us (different substituted benzenes, alcohols, carbon tetrachloride) the introduction of a suitably oriented analyzer decreased the intensity of the coherent background by not less than 10^3 times. In inorganic liquids (water, simple acids) this decrease was even more appreciable—up to 10^4 times. These data, which attest to the high degree of linearity of the polarization of the anti-Stokes ARS signal allow us to conclude that in the investigated media the imaginary part of the electronic susceptibility $\chi^{(3)NR}$ is small and apparently does not exceed 2–5% of the real part (otherwise the ARS background signal would have an appreciable elliptic polarization).

In all the investigated media the maximum increase of the contrast of the active spectra was reached, in accord with expression (10), when the angle between the pump-wave polarization planes was set at $\varphi\approx 60°$. The contrast (i.e., the intensity ratio of the anti-Stokes signals at the line center and on the wing increased in this case by 30–50 times for the polarized RS lines and by up to 20 times for the depolarized lines. Incidentally, owing to the weakness of the depolarized lines their contrast can far from always be measured without suppressing the coherent background. The contrasts of the 1178 cm^{-1} line of benzene and of the 760–790 cm^{-1} doublet of CCl_4, which have anomalous polarization characteristics,[38] increased insignificantly when the analyzer was introduced (see Sec. 3 below).

In the analysis of a gas mixture—nitrogen (buffer) and CO_2 (impurity)—the use of the polarization procedure has made it possible to increase by not less than 10 times the ARS sensitivity in the determination of the impurity concentration and to bring it up to 100 ppm CO_2.[31] Further increase of the sensitivity was limited in this case by the depolarizing influence of the windows of the cell containing the gas mixture, and the weakness of the registered signal. Elimination of these factors should increase the sensitivity of the CO_2 determination to the level 0.1 – 10 ppm.

As already shown in Sec. 2.1, measurement of the degree of depolarization of the RS lines with the aid of ARS has the distinguishing feature that the value $\bar{\rho}=\bar{\chi}^{(3)R}_{1221}/\chi^{(3)R}_{1111}$ obtained from the active spectra coincides with the value of ρ in spontaneous RS only when the RS tensor has no antisymmetrical part; conversely, a disparity between $\bar{\rho}$ and ρ attests to the presence of an anti-symmetrical component and, in accord with (4),

$$^1/_3 g_a^2/(b^2+^4/_{45}g^2)=\rho-\bar{\rho}. \tag{15}$$

As we shall see in Sec. 3, the simplest method of determining $\bar{\rho}$ is coherent ellipsometry, but with the aid of amplitude ARS it is possible to estimate $\bar{\rho}$ with sufficient accuracy. It is possible to measure for this purpose, for example, the ratio λ_R/λ_{NR} for two cases: 1) the polarization vectors of the pump waves are parallel and 2) they are perpendicular to each other.

For the arrangement 1) we obtain with the aid of (1)

$$(\lambda_R/\lambda_{NR})_\parallel=\bar{\chi}^{(3)R}_{1111}/\chi^{(3)NR}_{1111},$$

and analogously for the case 2) we have

$$(\lambda_R/\lambda_{NR})_\perp=3\bar{\chi}^{(3)R}_{1221}/\chi^{(3)NR}_{1111};$$

this yields $\bar{\rho}$:

$$\bar{\rho}=\bar{\chi}^{(3)R}_{1221}/\bar{\chi}^{(3)R}_{1111}={}^1/_3(\lambda_R/\lambda_{NR})_\perp/(\lambda_R/\lambda_{NR})_\parallel. \tag{16}$$

Figure 4 shows the dispersion curves $|\lambda(\Delta)|^2$ near the

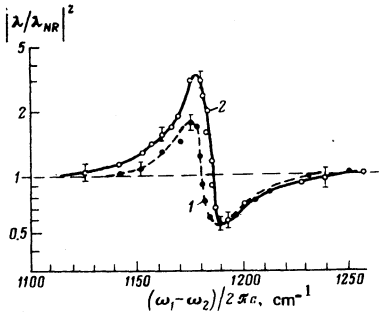

FIG. 4. Dispersion of anti-Stokes ARS signal in benzene ($\Omega/2\pi c=1178$ cm^{-1} line) for different pump-wave polarizations: 1) $\varphi=0$ (pump-wave polarization unit vectors parallel, $\mathbf{e}_1\parallel\mathbf{e}_2$); 2) $\varphi=90°$ ($\mathbf{e}_1\perp\mathbf{e}_2$).

not-fully-symmetrical line $\Omega/2\pi c = 1178$ cm^{-1} of benzene for the two indicated polarization configurations. From these data we obtain with the aid of (16) the estimates

$$\rho = 0.5 \pm 0.1, \quad \chi_{1111}^{(3)R}/\chi_{1111}^{(3)NR} = 0.7 \pm 0.2.$$

It is known from the spectra of the spontaneous RS that the degree of depolarization of this line is anomalously large: $\rho = 0.83 \pm 0.02$,[36] pointing to an appreciable contribution made to its intensity by the antisymmetrical part of the RS tensor. We see that the ARS data confirm this conclusion (see also Sec. 3).

3. COHERENT ELLIPSOMETRY OF RAMAN SCATTERING OF LIGHT IN ISOTROPIC MEDIA

3.1. As already indicated, in coherent Raman ellipsometry one measures the dispersion of the parameters of the elliptic polarization of the anti-Stokes signal at the frequency $\omega_a = 2\omega_1 - \omega_2$ as $\omega_1 - \omega_2$ is scanned. It can be seen from (1) that the onset of elliptic polarization of the anti-Stokes signal when linearly polarized pump waves interact at $\omega_1 - \omega_2 \approx \Omega$ is due to the non-collinearity of $\mathbf{P}_{NR}$ and $\mathbf{P}_R$ and to the presence of a phase shift in $\mathbf{P}^{(3)R}(\omega_a)$ relative to $\mathbf{P}^{(3)NR}(\omega_a)$, due to the complex character of $\chi_{1111}^{(3)R}$ near the Raman resonance. This explains, in particular, the dispersion of the plane of the polarization of the ARS signal near strong RS lines.[7]

An important feature of coherent ellipsometry is the independence of the polarization state of the registered signal of the intensity of the pump waves, a feature that rids this system immediately of a source of strong fluctuations. This is particular-valuable when pulsed lasers are used with intensities that experience, as a rule, appreciable fluctuations, whereas the state of polarization of their radiation can be reliably controlled.

3.2. *Principle of coherent ellipsometry*. The character of the dispersion of the parameters of the elliptic polarization of an anti-Stokes signal can be understood by considering the simple case of a solitary Raman resonance. It is convenient to analyze the polarization state of monochromatic waves with the aid of the so-called Poincaré sphere.[37] Each wave with elliptic polarization specified by an ellipse major-axis orientation ψ and by a degree of ellipticity $\chi = \pm \tan^{-1}(b/a)$ (b and a are respectively the minor and major semiaxes of the polarization ellipse) is set in correspondence with a point on a Poincaré sphere, with spherical coordinates 2ψ and 2χ; the value $\chi > 0$ is assigned to an ellipse with right-hand rotation, and $\chi < 0$ to an ellipse with left-hand rotation (see Fig. 5).

If the origin of the spherical coordinates ($2\psi = 0, 2\chi = 0$) is placed at a point on the Poincaré-sphere equator corresponding to the orientation of the vector $\mathbf{P}_{NR}$, then the polarization ellipse of the anti-Stokes signal can be specified with the aid of (1)–(3) by the following equations:

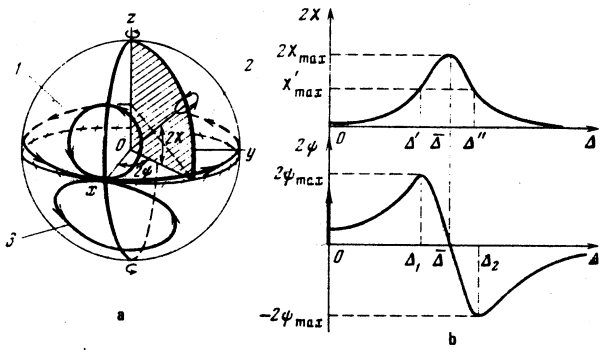

FIG. 5. Principle of coherent Raman ellipsometry. a) Representation of the polarization state of the coherently scattered anti-Stokes signal with the aid of a Poincare sphere: $1 - \alpha \sin\theta = 0.3$, $2 - \alpha \sin\theta = 1.0$, $3 - \alpha \sin\theta = -0.6$. b) Calculated curves that demonstrate the variation of the dispersion of the ellipticity (2χ) and the inclination angle of the major axis of the ellipse (2ψ) at $\alpha \sin\theta < 1$ (solitary Raman resonance with Lorentz shape). Coordinates; $\bar{\Delta} = \alpha \cos\theta$, $\Delta'_{,''} = \alpha\cos\theta \mp (1 + \alpha^2 \sin^2\theta)^{1/2}$, $2\psi_{max} = \tan^{-1}[\alpha \sin\theta/(1 - \alpha^2 \sin^2\theta)^{1/2}]$, $\Delta_{1,2} = \alpha\cos\theta \mp (1 - \alpha^2 \sin^2\theta)^{1/2}$, $2\chi_{max} = \sin^{-1}[2\alpha \sin\theta/(1 + \alpha^2 \sin^2\theta)]$.

$$\operatorname{tg} 2\psi = -2\alpha \sin\theta(\Delta - \alpha\cos\theta)/[(\Delta - \alpha\cos\theta)^2 + 1 - \alpha^2 \sin^2\theta], \quad (17)$$

$$\sin 2\chi = 2\alpha \sin\theta/[(\Delta - \alpha\cos\theta)^2 + 1 + \alpha^2 \sin^2\theta], \quad (18)$$

here

$$\alpha = \frac{\chi_{1111}^{(3)R}}{\chi_{1111}^{(3)NR}} \frac{|\mathbf{P}_R|}{|\mathbf{P}_{NR}|}, \quad \chi_{1111}^{(3)R} = \frac{NL^4}{24M\Omega\Gamma}\left(b^2 + \frac{4}{45}g^2\right);$$

the angle θ is defined in (9). By eliminating the parameter Δ from (17) and (18) and by transforming the spherical coordinates via rotation through an angle $\gamma = \pi/2 - \chi_{max}$ around the y axis, where

$$\sin 2\chi_{max} = \frac{2\alpha \sin\theta}{1 + \alpha^2 \sin^2\theta}, \quad (19)$$

it is easy to verify that (17) and (18) define a circle tangent to the equator and have a center at the point with coordinates $2\chi = \chi_{max}$, $2\psi = 0$. These circles are shown in Fig. 5a for different values of the parameter $\alpha \sin\theta$.

The direction of rotation in the signal polarization ellipse is determined by the sign of $\alpha \sin\theta$; this sign is different for the isotropic and anisotropic components of the source $\mathbf{P}^{(3)}(\omega_a)$.

Equation (19) determines the maximal signal ellipticity, reached at $\Delta = \alpha\cos\theta$, with $2\psi = 0$ or $2\psi = \pi$. If $|\alpha \sin\theta| \leq 1$, then the maximum rotation angle of the major axis of the ellipse, $2\psi_{max}$, which is determined from the relation

$$\pm 2\psi_{max} = \operatorname{arctg}\{\alpha \sin\theta/(1 - \alpha^2 \sin^2\theta)^{1/2}\}, \quad (20)$$

is reached at $\Delta_{1,2} = \alpha\cos\theta \mp (1 - \alpha^2 \sin^2\theta)^{1/2}$ (see Fig. 5b). At $|\alpha \sin\theta| > 1$, the major semiaxis of the ellipse is rotated through π.

At $|\alpha \sin\theta| \ll 1$ the angles ψ and χ are small, and the shapes of the resonance curves $\psi(\Delta)$ and $\chi(\Delta)$ coincide in this case with the dispersion contours of the real and imaginary parts of $\chi_{1111}^{(3)R}(\Delta)$, respectively, but the centers of the former curves are shifted from the center

of the Raman resonance ($\Delta = 0$) by an amount $\bar{\Delta} = \alpha\cos\theta$. Indeed, assuming in (17)–(18) $\alpha\sin\theta \ll 1$ and putting $\Delta' = \Delta - \alpha\cos\theta$, and then making the substitutions $\tan 2\psi \approx 2\psi$ and $\sin 2\chi \approx 2\chi$, we obtain

$$\psi = -\alpha\sin\theta\frac{\Delta'}{1+(\Delta')^2} \sim \mathrm{Re}\,\chi^{(3)R}(\Delta'),$$

$$\chi = \alpha\sin\theta\frac{1}{1+(\Delta')^2} \sim \mathrm{Im}\,\chi^{(3)R}(\Delta').$$

We note that the condition $|\alpha\sin\theta| \ll 1$ can always be satisfied, no matter how large α may be, by decreasing the angle φ between the pump polarization unit vectors, and accordingly decreasing $\sin\theta$.

Thus, coherent ellipsometry permits separate measurement of the dispersion of the real and imaginary parts of $\chi^{(3)}(\omega_a; \omega_1, \omega_1, -\omega_2)$ in the vicinity of a solitary resonance of Lorentz shape.

In the latter case it is easy to determine the parameter $\bar{\rho} = \bar{\chi}^{(3)R}_{1221}/\bar{\chi}^{(3)NR}_{1111}$ introduced in (4). From the parameters $\alpha\sin\theta$ and $\alpha\cos\theta$ measured from the polarization spectra we determine $\tan\theta$, and then from formula (9) we get $\bar{\rho}$.

The value of $\bar{\rho}$ can also be calculated if one knows $\bar{\chi}^{(3)R}_{1111}/\chi^{(3)NR}_{1111}$ from the spectrum of the amplitude ASR and $\alpha\sin\theta$ is determined from the polarization spectra, so that

$$\alpha\sin\theta = \frac{3\bar{\chi}^{(3)R}_{1111}}{2\chi^{(3)NR}_{1111}}\frac{(3\bar{\rho}-1)\sin 2\varphi}{8\cos^2\varphi+1}. \qquad (21)$$

3.3. *Polarization spectra of Raman resonances of arbitrary shape.* In the case of an arbitrary shape at $\max|P^{(3)}_R| \ll |P^{(3)}_{NR}|$ (i.e., $|\alpha| \ll 1$), χ and ψ are small and, just as in the simplest case of a solitary line, we again have

$$\psi(\omega_1-\omega_2) \sim \mathrm{Re}\,\chi^{(3)}_{1111}(\omega_a; \omega_1, \omega_1, -\omega_2),$$

$$\chi(\omega_1-\omega_2) \sim \frac{b}{a}(\omega_1-\omega_2) \sim \mathrm{Im}\,\chi^{(3)}_{1111}(\omega_a; \omega_1, \omega_1, -\omega_2).$$

At $|\alpha| \geq 1$, however, no such simple relations are obtained even if $|\sin\theta| \ll 1$. In the general case the following equations are valid:

$$\mathrm{tg}\,2\psi(\Delta) = \frac{|P^{(3)}_R(\Delta)|^2\sin 2\theta + 2P_{NR}\sin\theta\,\mathrm{Re}[P^{(3)}_R(\Delta)]}{|P^{(3)}_R(\Delta)|^2\cos 2\theta + 2\cos\theta\,P_{NR}\,\mathrm{Re}[P^{(3)}_R(\Delta)] + P_{NR}^2}, \qquad (22)$$

$$\sin 2\chi(\Delta) = 2P_{NR}\sin\theta\frac{\mathrm{Im}[P^{(3)}_R(\Delta)]}{|P^{(3)}_R(\Delta)|^2 + 2\cos\theta P_{NR}\,\mathrm{Re}[P^{(3)}_R(\Delta)] + P_{NR}^2} \qquad (23)$$

where

$$\mathbf{P}^{(3)}_R(\Delta) = P^{(3)}_R(\Delta)\mathbf{P}_R, \quad P_{NR} = |\mathbf{P}_{NP}|.$$

Here, just as in amplitude ARS, interference phenomena are possible within inhomogeneously broadened band produced by superimposed lines having different polarization characteristics.

3.4. *Experimental setup.* All the main elements of the experimental setup for coherent Raman ellipsometry are the same as in the case of amplitude ASR (see Fig. 3). Now, however, a phase plate of variable thickness is placed in the path of the anti-Stokes component beam, to compensate for the phase difference between the orthogonal polarizations. We used for this purpose an ordinary calcite rotating Berek compensator.[38] It is very important that in this case there is no longer any need for using two additional reference channels, since there is no need to normalize the registered signal to the intensities of the pump waves.

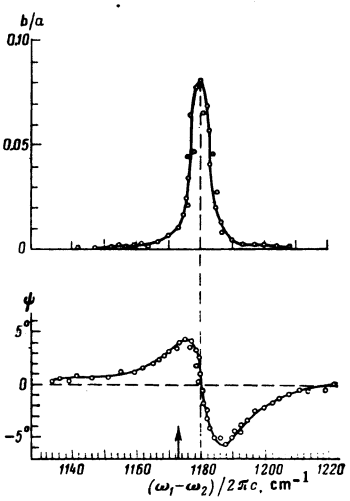

FIG. 6. Dispersion of the polarization parameters of the anti-Stokes ASR signal in benzene; the arrow marks the position of the center of the spontaneous RS line: $\varphi = 61°$.

3.5. *Experimental results.* The results of the experiments performed by the method of coherent Raman ellipsometry are shown in Figs. 6–8.

Figure 6 shows the experimental dispersion curves for the parameters b/a and ψ near the 1178 cm^{-1} line in benzene. Notice should be taken of the insignificant scatter of the experimental points. The angle measurement accuracy in our experiments was not worse than 10^{-2} rad. Under these conditions, the dispersion of $\chi^{(3)R}$ can be measured with the same accuracy, and it is not difficult to improve the accuracy by two orders, especially if cw lasers are used.

The measurement results shown in Fig. 6 have confirmed the conclusion that the RS tensor has appreciable asymmetry (cf. Sec. 2.5) for the investigated line.

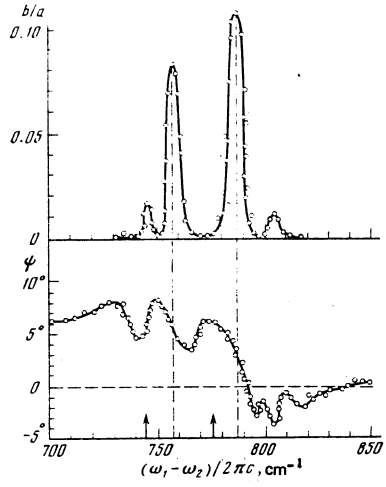

FIG. 7. Dispersion of the polarization parameters of the anti-Stokes ASR signal in liquid CCl_4. The arrows mark the positions of the centers of the principal components of the Fermi doublet in spontaneous RS. The isotopic structure of the spectrum can be seen; $\varphi = 59°$.

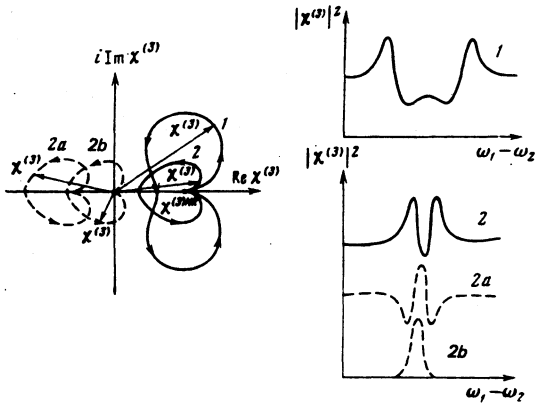

FIG. 8. Diagram explaining the principle of the resolution of the doublet of superimposed lines in ASR. Left—representation of cubic susceptibility on the complex plane, right—dispersion curves of $|\chi^{(3)}|^2$ corresponding to the curves 1 and 2 shown on the left.

We have for this line

$$\bar{\rho}=0.42\pm0.02,$$

$$\chi^{(3)R}_{1111}/\chi^{(3)NR}_{1111}=0.7\pm0.1.$$

We recall that in spontaneous RS the degree of depolarization of this line is $\rho=0.83$. From this and from (15) we have

$$g_a^2/3(b^2+{}^4/_{15}g^2)=\rho-\bar{\rho}\approx0.4.$$

We note that the spectral resolution here and in the subsequent measurements was limited by the line width of the tunable laser, $\Delta\nu=2.5$ cm^{-1}.

Figure 7 shows the dispersion curves of the polarization parameters of an anti-Stokes signal in liquid CCl_4 near the Fermi doublet 760–790 cm^{-1}, which also has anomalous polarization characteristics.[36] With the aid of these curves, and also be measuring the shift of the peaks of the ellipticity of the principal components of the doublet from the spontaneous RS centers measured by us with the same setup for the purpose of finding $\alpha\cos\theta$, we have determined the following: for the 757 cm^{-1} component:

$$\alpha\sin\theta=0.083,\quad \alpha\cos\theta=1.4,$$

$$\bar{\rho}_1=0.38\pm0.04,\quad \chi^{(3)R}_{1111}/\chi^{(3)NR}_{1111}=1.4\pm0.3;$$

b) for the 787 cm^{-1} component:

$$\alpha\sin\theta=0.11,$$

$$\alpha\cos\theta=1.0,$$

$$\bar{\rho}_2=0.42\pm0.04,$$

$$\chi^{(3)R}_{1111}/\chi^{(3)NR}_{1111}=1.0\pm0.3.$$

We see again that the values of $\bar{\rho}_{1,2}$ measured by coherent ellipsometry for these lines are much lower than the degrees of depolarization measured in spontaneous RS: $\rho_{1,2}\approx0.8$. This also attests to the asymmetry of the RS tensors associated with these lines.[36]

The described procedure was applied by us also to an investigation of a number of strong fully symmetrical lines in benzene and in mesitylene;[39] here the experimentally determined values of $\bar{\rho}$ agreed within the limits of the measurement accuracy with the values of ρ determined from the spontaneous RS spectrum.

The capabilities of the coherent-ellipsometry method are particularly clearly illustrated by the experimental results on the resolution of the RS line in concentrated nitric acid (HNO_3) with a central frequency $\Omega/2\pi c=1305$ cm^{-1} (see Fig. 2 of [33]).

Polarization spectra show clearly a fine structure. Since no such structure exists in the spontaneous spectra, one can speak of resolution of superimposed lines of unequal symmetry (see Sec. 4 below). Qualitative agreement is obtained here with the experimental data on SRS.[40]

4. RESOLUTION OF INTERNAL STRUCTURE OF INHOMOGENEOUSLY BROADENED LINE WITH THE AID OF POLARIZATION ASR

4.1. In Secs. 2.3 and 3.5 we have already touched upon the possibility of using polarization ARS to resolve the inhomgeneous structure of RS lines. The new factors that the polarization ARS introduces in the problem of resolution of superimposed lines are the possibilities of shaping the line contours and, accordingly, the control of the shape of the overallband, which is the result of interference of its constitutent lines.

We turn first to the simplest case of superposition of two Raman resonances of equal width, characterized by opposite signs of the resonant contributions to the summary cubic susceptibility:

$$\chi^{(3)}(\omega_a;\omega_1,\omega_1,-\omega_2)=\chi^{(3)NR}+\frac{|\bar{\chi}^{(3)R_1}|}{-i-\Delta}-\frac{|\bar{\chi}^{(3)R_2}|}{-i-(\Delta-a)};\qquad(24)$$

here $\Delta=(-\Omega_1+(\omega_1-\omega_2))/\Gamma$ is the detuning from the center of the first resonance, and $a=(\Omega_1-\Omega_2)/\Gamma$ is the distance between line centers, normalized to the half-width. We put for simplicity $|\bar{\chi}^{(3)R_1}|=|\bar{\chi}^{(3)R_2}|=\bar{\chi}^{(3)R}$.

It is convenient to analyze expression (24) by mapping the values of $\chi^{(3)}(\omega_a)$ on the complex plane (Fig. 8). When Δ is scanned from $-\infty$ to $+\infty$, the end point of the vector $\chi^{(3)}$ traces the curves numbered 1 and 2. Curve 1 corresponds to the case of two lines that can be resolved in accordance with the Rayleigh criterion: $a>2$. The behavior of $|\chi^{(3)}(\Delta)|^2$ is shown in Fig. 8 on the right. When the lines come closer together, the curve 1 is deformed and is transformed at $a=2$ into curve 2. (Depending on the magnitude and sign of $\chi^{(3)NR}$, the curves 1 and 2 shift along the abscissa axis, as shown dashed in Fig. 8.) The corresponding spectra are shown in Fig. 8 on the right. With further approach of the lines ($a<2$), curve 2 shrinks but retains its shape, so that the spectra of $|\chi^{(3)}(\Delta)|^2$ do not change qualitatively. This means that in the case under consideration two arbitrarily close lines, interfering, will always be resolved in the spectrum of the amplitude ASR.

The picture of the superposition of two lines of un-

equal intensity and width is more complicated,[41] but the general conclusion that they are resolvable by ASR remains in force.

We note that since coherent ellipsometry makes it possible to measure separately the dispersion of the real and imaginary parts of $\chi^{(3)}$, the statements made above (and illustrated in Fig. 8) pertain also to it (we have in mind lines with different signs of $\chi^{(3)R}$).

4.2. The prospect of resolving close lines in ordinary amplitude ASR are greatly limited because they call for a fortuitous combination of the signs of the resonant contributions from different lines to the cubic nonlinearity, and the possibility of resolving close lines is realized to full extent only in polarization ARS, where it becomes possible to control the sign of the ratio $\chi^{(3)R}/\chi^{(3)NR} = \lambda_R/\lambda_{NR}$ (see Sec. 2.3). As shown in Sec. 2.2, the level of the coherent background in the spectra of amplitude ARS can also be greatly reduced.

In coherent ellipsometry, the necessary combination of signs of the interfering lines is obtained whenever the parameters $\bar{\rho}_{1,2}$ of these lines satisfy the relations $\bar{\rho}_1 < 1/3, \bar{\rho}_2 > 1/3$ or, conversely, $\bar{\rho}_1 > 1/3, \bar{\rho}_2 < 1/3$.

4.3. We have already noted, with the broad 1305 cm^{-1} nitric-acid band as an example, that polarization active spectra are richer in details than the spectra obtained with the aid of spontaneous RS (Sec. 3.5). This undoubtedly attests to the inhomogeneous broadening of this line. The experimental results shown in Fig. 9 confirm this conclusion.

Curve 1 of Fig. 9 corresponds to the dispersion of the intensity of the anti-Stokes signal after passing through an analyzer set for suppression of the nondispersing electronic pedestal, i.e., set perpendicular to the vector $\mathbf{P}_{NR}$ (Fig. 1). The splitting of the spectrum of two components spaced ~ 20 cm^{-1} apart is clearly seen.

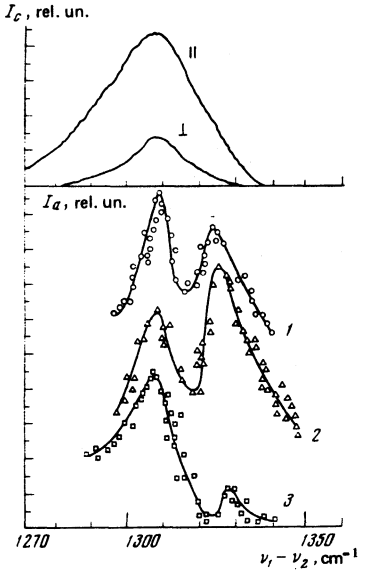

FIG. 9. Splitting of the amplitude ARS spectrum of concentrated nitric acid ($\Omega/2\pi c \approx 1305$ cm^{-1}) following introduction of an analyzer: 1—analyzer crossed with polarization of coherent background ($\epsilon = 0$); 2—analyzer rotated through angle $\epsilon = -5°$, polarized ($\bar{\rho}_1 < 1/3$) component of the doublet is suppressed; 3—analyzer rotated through angle $\epsilon = +5°$, the depolarized ($\bar{\rho}_2 > 1/3$) component of the doublet is suppressed. The upper part of the figure shows the polarized (∥) and the depolarized (⊥) spectra of the spontaneous RS.

Curves 2 and 3 of Fig. 9 demonstrate the deformation of the spectrum of the anti-Stokes signal when the transmission plane of the analyzer is rotated $\pm 5°$ relative to the position corresponding to curve 1. It can be concluded with their aid that the low-frequency component of the doublet (central frequency 1305 cm^{-1}) is characterized by the value $\bar{\rho} < 1/3$, as against $\bar{\rho} > 1/3$ for the high-frequency component (1325 cm^{-1}).

It can thus be stated that under the common contour of the 1305 cm^{-1} band of concentrated nitric acid there exist several lines of different symmetry, and these lines apparently correspond to different oscillations of the NO_2 group deformed under the influence of the hydrogen-bond forces (cf. [42]).

5. CONCLUSION

The polarization effects in coherent active Raman spectroscopy are quite varied and frequently have no analogs in spontaneous Raman spectroscopy. The last statement pertains to the suppression of the nondispersing pedestal, to the interference of various contributions to the susceptibility, and others. The dispersion of the polarization parameters of a coherently scattered signal within the limits of the Raman resonance contour yields much more information than the dispersion of the degree of depolarization measured in spontaneous Raman spectroscopy.[43]

Polarization ASR, on the one hand, makes it possible to improve considerably the methods used to measure the parameters of the RS line (particularly, to investigate the symmetry of the RS tensor), and on the other hand makes it possible to perform experiments quite inaccessible to spontaneous scattering spectroscopy—shaping of the Raman-resonance scattering, resolution of inhomogeneously broadened bands, separate measurements of the dispersion curves of the real and imaginary parts of the cubic susceptibility.

It is quite tempting here to use the methods of traditional ellipsometry, which are extremely accurate,[44] in an ARS scheme based on stabilized cw lasers.[11-13] The coherent ellipsometry method can be easily generalized to include measurement of the dispersion of cubic susceptibility in the vicinity of resonances of other types: one- and two-photon electron resonance, exciton resonances, and others.

The effect of dispersion of the polarization parameters of an anti-Stokes signal, which is the basis of coherent ellipsometry, can be used in an entirely different field—for example for the stabilization and exact determination of the wavelength of a tunable laser, since the independence of the effect of the intensity makes it possible to tie-in the frequency of the tunable source with the aid of standard Raman lines in a wide spectral range.

In connection with the methods discussed in Sec. 2.2 for suppressing the coherent background in amplitude active spectra, it must be noted that the main idea of separating the resonant and nonresonant processes on the basis of polarization is quite general. For example, its possible to attempt to discriminate on this basis the coherent background in active hyper-Raman spectroscopy,[45] as well as in other types of four-photon coherent spectroscopy.[5] Just as in amplitude ARS, satisfaction of the Kleinman relations (A.6) for the components of the nonresonant component of the susceptibility $\chi^{(3)}$ is not at all obligatory. Even if the tensor $\chi^{(3)NR}_{ijkl}$ is complex and the background radiation generated by it is elliptically polarized, discrimination is still possible with the aid of a phase plate that complements the phase difference between the polarized components of the background radiation to 0 or π, and an analyzer placed behind the phase plate to block the outgoing linearly polarized light wave. The part of the radiation produced by the resonant component $\chi^{(3)}_{ij}$ of the cubic susceptibility will pass through this analyzer, since its polarization ellipse on emerging from the investigated medium is generally speaking different from the polarization ellipse of the coherent background.

In conclusion, we note the following. Throughout this article, when speaking of ASR, we had in mind the process easiest to realize, in the form $\omega_a = 2\omega_1 - \omega_2$. For complete measurements it is necessary, however, to use in polarization ARS a nondegenerate four-photon process of the type $\omega_a = \omega + \omega_1 - \omega_2$, $\omega \neq \omega_1, \omega_2$. Only then will three of the nonzero components of the tensor $\chi^{(3)R}_{ijkl}(\omega_a; \omega, \omega_1, -\omega_2)$ be independent, and separate measurements of these three will suffice for an independent determination of the three invariants b^2, g^2, and g_a^2 of the RS tensor; in this case there is no need to resort to spontaneous RS data.

The authors thank I. A. Yakovlev and R. Yu. Orlov for supplying the polarization devices and for a discussion of the ellipsometry methods, and to I. L. Shumai, F. N. Gadzhiev, M. G. Karimov, and M. L. Sybeva for help with the individual experiments.

APPENDIX

CUBIC-SUSCEPTIBILITY TENSOR OF ANISOTROPIC RAMAN-ACTIVE MEDIUM-CONNECTION WITH THE INVARIANTS OF THE RAMAN-SCATTERING TENSOR

The processes that occur in coherent ARS in a centrosymmetric medium are described within the framework of a phenomenological expansion of the nonlinear polarization by the term cubic in the field:

$$P_i^{(3)}(\omega_a) = 3\chi^{(3)}_{ijkl}(\omega_a; \omega_1, \omega_1, -\omega_2) E_j^{(1)} E_k^{(1)} E_l^{(2)*}. \quad (A.1)$$

Here $E_j^{(1)}$ and $E_l^{(2)}$ are the Cartesian components of the amplitudes of plane pump waves with respective frequencies ω_1 and ω_2; $\omega_a = 2\omega_1 - \omega_2$; the summation convention is used. In an isotropic medium (liquid, gas) the spatial symmetry limits the number of nonzero components of the cubic-susceptibility tensor to the following (see, e.g.,[3,46]):

$$\chi^{(3)}_{iiii}(\omega_a; \omega_1, \omega_1, -\omega_2), \quad \chi^{(3)}_{iijj}(\omega_a; \omega_1, \omega_1, -\omega_2) = \chi^{(3)}_{ijji}(\omega_a; \omega_1, \omega_1, -\omega_2),$$
$$\chi^{(3)}_{ijij}(\omega_a; \omega_1, \omega_1, -\omega_2). \quad (A.2)$$

Only two of these 21 components are independent,[5)] since

$$\chi^{(3)}_{iiii}(\omega_a; \omega_1, \omega_1, -\omega_2) = 2\chi^{(3)}_{iijj}(\omega_a; \omega_1, \omega_1, -\omega_2) + \chi^{(3)}_{ijji}(\omega_a; \omega_1, \omega_1, -\omega_2). \quad (A.3)$$

In an isotropic medium, taking (A.2) and (A.3) into account, expression (A.1) can be written in a simple vector form (see[47]):

$$\mathbf{P}^{(3)}(\omega_a) = 3\{2\chi^{(3)}_{1122}(\omega_a; \omega_1, \omega_1, -\omega_2)\mathbf{E}^{(1)}(\mathbf{E}^{(1)}\mathbf{E}^{(2)*}) + \chi^{(3)}_{1221}(\omega_a; \omega_1, \omega_1, -\omega_2)\mathbf{E}^{(2)*}(\mathbf{E}^{(1)}\mathbf{E}^{(1)})\}. \quad (A.4)$$

In the transparency region of the medium, near the Raman resonance (i.e., at $\omega_1 - \omega_2 \approx \Omega$, where Ω is the frequency of the molecular vibration that is active in RS), $\chi^{(3)}$ breaks up into a "nonresonant" electronic nondispersing part (See Sec. 1) $\chi^{(3)NR}_{ijkl}(\omega_a; \omega_1, \omega_1, -\omega_2)$ and a resonant part $\chi^{(3)R}_{ijkl}(\omega_a; \omega_1, \omega_1, -\omega_2)$, which has a strong frequency dependence. Under conditions when Placek's polarizability theory is valid[25] we can write (see e.g., expression (6) of [8]):

$$\chi^{(3)R}_{ijkl}(\omega_a; \omega_1, \omega_1, -\omega_2) = \frac{NL^4}{24M\Omega\Gamma}\left\langle \left(\frac{\partial\alpha_{ij}}{\partial Q}\right)_0 \left(\frac{\partial\alpha_{kl}}{\partial Q}\right)_0 \right\rangle D(\Omega, \omega_1 - \omega_2). \quad (A.5)$$

Here $(\partial\alpha_{ij}/\partial Q)_0$ is the RS tensor connected with the preferred vibration, M is the reduced mass of the molecule, N is the molecule density; $L = (\epsilon + 2)/3$ is the Lorentz correction factor for the internal field, Γ is half-width of the resonance curve of the molecular vibration:

$$D(\Omega, \omega_1 - \omega_2) = \frac{2\Omega\Gamma}{\Omega^2 - 2i\Gamma(\omega_1 - \omega_2) - (\omega_1 - \omega_2)^2} \approx \frac{1}{-i - \Delta}, \quad \Delta = \frac{\omega_1 - \omega_2 - \Omega}{\Gamma};$$

the angle brackets denote averaging over the orientations

The macroscopic and molecular symmetry impose different limitations on the components of the tensors $\chi^{(3)R}_{ijkl}$ and $\chi^{(3)NR}_{ijkl}$, owing to the different character of the excitation of the ionic and electronic subsystems. In the absence of one- and two-photon resonances, the excitation of the electronic subsystem is not connected with energy dissipation processes, since only virtual transitions are excited, and the Kleinman relations,[46,48] which lead in an isotropic medium to essentially only one real independent component $\chi^{(3)NR}_{ijkl}$: $\chi^{(3)N}_{ijkl}$ satisfies

$$\chi^{(3)NR}_{1111}(\omega_a; \omega_1, \omega_1, -\omega_2) = 3\chi^{(3)NR}_{1122}(\omega_a; \omega_1, \omega_1, -\omega_2) = 3\chi^{(3)NR}_{1221}(\omega_a; \omega_1, \omega_1, -\omega_2). \quad (A.6)$$

On the other hand, in the nuclear system there are excited real motions, which cause the incident light wave to lose energy, so that the Kleinman relations are not satisfied for $\chi^{(3)R}_{ijkl}$, so that in accordance with (A.3) we have

$$\chi^{(3)R}_{1111} = 2\chi^{(3)R}_{1122} + \chi^{(3)R}_{1221} \quad (A.7)$$

and generally speaking $\chi^{(3)R}_{1122}(\omega_a; \omega_1, \omega_1, -\omega_2) \neq \chi^{(3)R}_{1221}(\omega_a; \omega_1, \omega_1, -\omega_2)$, in which case the components $\chi^{(3)R}_{ijkl}$ are

complex.

With the aid of the averaging procedure described in[8] we can obtain the following expressions that relate the nonzero components of the tensor $\chi^{(3)R}_{ijkl}$ with the invariants of the molecular RS tensor

$$\chi^{(3)R}_{1111}(\omega_a;\omega_1,\omega_1,-\omega_2)=\frac{NL^4}{24M\Omega\Gamma}\left(b^2+\frac{4}{45}g^2\right)\frac{1}{-i-\Delta}, \quad (A.8)$$

$$\chi^{(3)R}_{1122}(\omega_a;\omega_1,\omega_1,-\omega_2)=\frac{NL^4}{24M\Omega\Gamma}\left(\frac{1}{2}b^2+\frac{1}{90}g^2+\frac{1}{12}g_a^2\right)\frac{1}{-i-\Delta}, \quad (A.9)$$

$$\chi^{(3)R}_{1221}(\omega_a;\omega_1,\omega_1,-\omega_2)=\frac{NL^4}{24M\Omega\Gamma}\left(\frac{1}{15}g^2-\frac{1}{6}g_a^2\right)\frac{1}{-i-\Delta}. \quad (A.10)$$

Here $b=1/3\mathrm{Sp}(\partial\alpha_{ik}/\partial Q)_0=1/3(\alpha_1+\alpha_2+\alpha_3)$ is the average polarizability, which determines the scalar (isotropic Raman scattering;

$$g^2=3/2[\mathrm{Sp}\{(\partial\alpha_{ik}/\partial Q)_0^2\}-3b^2]=1/2[(\alpha_1-\alpha_2)^2+(\alpha_2-\alpha_3)^2+(\alpha_1-\alpha_3)^2]$$

is the anisotropy with which the quadrupole (anisotropic) RS is connected ($\alpha_{1,2,3}$ are the principal values of the symmetric part of the RS tensor);

$$g_a^2=-\frac{1}{4}\mathrm{Sp}\left\{\left[\left(\frac{\partial\alpha_{ik}}{\partial Q}\right)_0-\left(\frac{\partial\alpha_{ki}}{\partial Q}\right)_0\right]^2\right\}=\frac{1}{2}\left\{\left[\left(\frac{\partial\alpha_{12}}{\partial Q}\right)_0-\left(\frac{\partial\alpha_{21}}{\partial Q}\right)_0\right]^2+\left[\left(\frac{\partial\alpha_{13}}{\partial Q}\right)_0-\left(\frac{\partial\alpha_{31}}{\partial Q}\right)_0\right]^2+\left[\left(\frac{\partial\alpha_{23}}{\partial Q}\right)_0-\left(\frac{\partial\alpha_{32}}{\partial Q}\right)_0\right]^2\right\}$$

is an invariant that characterizes the antisymmetrical component of the RS tensor and the R connected with the magnetic dipole (antisymmetrical) RS.

[1)]A particularly extensively used scheme is one in which scattering of radiation at a frequency $\omega_a=2\omega_1-\omega_2$ ($\omega=\omega_1$) is registered. This in fact is the nonlinear-spectroscopy variant customarily designated CARS (coherent spectroscopy of anti-Stokes scattering). We use here, nontheless, the more inclusive term "active spectroscopy" introduced in the USSR.[6] Even if the situation involves only coherent effects, anti-Stokes spectroscopy does not provide exhaustive information on the medium. In a number of cases, especially under conditions of double and triple resonances (see[3]), the Stokes component carries additional information; furthermore, schemes with $\omega\neq\omega_1$ and $\omega\neq\omega_2$ are being more frequently used of late (the so-called three-frequency ARS scheme, see[6] and the material of the present article).

[2)]An investigation of the Raman spectrum of water by the amplitude ARS method[21] has in fact yielded no new information compared with spontaneous-scattering spectroscopy.

[3)]Expression (2) is valid if the Kleinman relations (A.6) are rigorously satisfied. In the opposite case we have

$$P_{NR}=3\left\{2\left[\frac{\chi^{(3)NR}_{1122}(\omega_a;\omega_1,\omega_1,-\omega_2)}{\chi^{(3)NR}_{1111}(\omega_a;\omega_1,\omega_1,-\omega_2)}\right]e_1(e_1e_2^*)+\frac{\chi^{(3)NR}_{1221}(\omega_a;\omega_1,\omega_1,-\omega_2)}{\chi^{(3)NR}_{1111}(\omega_a;\omega_2,\omega_1,-\omega_2)}e_2^*(e_1e_1)\right\} \quad (2a)$$

[4)]In the calculation of the polarization dependence of an anti-Stokes signal generated by the anisotropic component of the tensor $\chi^{(3)R}_{ijkl}$, an error has crept into[34a]—cf. formula (8) of the present paper as well as Table 1 of[34a].

[5)]In ARS with nondegenerate frequencies, i.e., in the scheme $\omega_a=\omega+\omega_1-\omega_2$, $\omega\neq\omega_1,\omega_2$, the tensor $\chi^{(3)R}_{ijkl}(\omega_a;\omega,\omega_1,-\omega_2)$ has three independent components.

[1]R. Shen, Rev. Mod. Phys. **48**, 1 (1976).
[2]V. S. Letokhov, Usp. Fiz. Nauk **118**, 199 (1976) [Sov. Phys. Usp. **19**, 109 (1976)].
[3]S. A. Akhmanov and N. I. Koroteev, Usp. Fiz. Nauk **123**, 405 (1977) [Sov. Phys. Usp. **20**, 899 (1977)].
[4]M. Maier, Appl. Phys. **11**, 209 (1976).
[5]Ninth Intern. Conf. on Quantum Electronics, Amsterdam, 1976, Digest of Technical Papers, Opt. Commun. **18**, No. 1 (1976); Tunable Lasers and Application, eds. A. Mooradian, T. Jaeger, and P. Stokseth, Springer, Berlin-Heidelberg-New York, 1976.
[6]S. A. Akhmanov, V. G. Smitriev, A. I. Kovrigin, N. I. Koroteev, V. G. Tunkin, and A. I. Kholodnykh, Pis'ma Zh. Eksp. Teor. Fiz. **15**, 600 (1972) [JETP Lett. **15**, 425 (1972)].
[7]M. Levenson and N. Bloembergen, Phys. Rev. B **10**, 4447 (1974).
[8]S. A. Akhmanov and N. I. Koroteev, Zh. Eksp. Teor. Fiz. **67**, 1306 (1974) [Sov. Phys. JETP **40**, 650 (1975)].
[9]R. L. Byer, R. F. Begley, and A. B. Harvey, Appl. Phys. Lett. **25**, 387 (1974).
[10]J. P. Taran, in: Tunable Lasers and Application, eds. A. Mooradian, T. Jaeger, and P. Stoksets, Springer, Berlin-Heidelberg-New York, 1976.
[11]S. A. Akhmanov, N. I. Koroteev, R. Yu. Orlov, and I. L. Shumaĭ, Pis'ma Zh. Eksp. Teor. Fiz. **23**, 276 (1976) [JETP Lett. **23**, 249 (1976)]; F. N. Gadzhiev, N. I. Koroteev, R. Yu. Orlov, and I. L. Shumaĭ, Paper at All-Union Conference on Nonlinear Resonant Processes, Krasnoyarsk, September, 1977.
[12]V. I. Fabelinskii, B. B. Krynetskii, L. A. Kulevskii, V. A. Mishin, A. M. Prokhorov, A. D. Saveliev, and V. V. Smirnov, Opt. Commun. **20**, 389 (1977); **21**, 225 (1977).
[13]R. L. Byer, Paper at Fifth Vavilov Conf. on Nonlinear Optics, Novosibirsk, June, 1977.
[14]S. A. Akhmanov and N. I. Koroteev, Theory of light scattering in condensed matter, eds. J. Birman, B. Bendow, and V. M. Agranovitch, Plenum Press, New York, 1976, p. 241.
[15]A. F. Bunkin, S. G. Ivanov, and N. I. Koroteev, Pis'ma Zh. Eksp. Teor. Fiz. **24**, 468 (1976) [JETP Lett. **24**, 429 (1976)].
[16]R. T. Linch and H. Lotem, J. Chem. Phys. **66**, 1905 (1977).
[17]J. Nestor, T. G. Spiro, and G. Klaumnitzer, Proc. Natl. Acad. Sci. USA **73**, 3329 (1976).
[18]T. Carreira, T. Maguerre, and B. Malloy, J. Chem. Phys. **66**, 2621 (1977).
[19]T. R. Lynch, S. D. Kramer, H. Lotem, and N. Bloembergen, Opt. Commun. **16**, 372 (1976).
[20]N. Bloembergen, S. D. Kramer, and F. G. Parsons, Phys. Rev. B **9**, 1853 (1974).
[21]I. Itzkan and D. A. Leonard, Appl. Phys. Lett. **26**, 106 (1975).
[22]A. Owyong and P. S. Peercy, J. Appl. Phys. **48**, 674 (1977).
[23]D. Heiman, R. W. Hellwarth, M. D. Levensen, and G. Martin, Phys. Rev. Lett. **36**, 189 (1976).
[24]A. Owyong, Post Deadline Paper presented on the Conf. on Laser Engineering and Applications, Washington, May, 1977; Opt. Commun. **22**, 323 (1977).
[25]Placzek, Raleigh and Raman Scattering, Lawrence Rad. Lab. Livermore, Calif. 1959 (Transl. from Handuch d. Radiologie, 1934, Russ. transl. ONTI, 1934).
[26]G. Herzberg, Virbrational and Rotational Spectra of Polyatomic Molecules, Van Nostrand, 1945.
[27]M. M. Sushchinskiĭ, Spektry kombinatsionnogo rasseyaniya molekul i kristallov (Raman Spectra of Molecules and Crystals), Nauka, 1969.
[28]C. Wieman and T. Hänsch, Phys. Rev. Lett. **36**, 1170 (1976); R. Teets, R. Feinberg, T. W. Hänsch, and A. L. Shawlow, Phys. Rev. Lett. **37**, 683 (1976).
[29]A. F. Bunkin, S. G. Ivanov, and N. I. Koroteev, Paper at Seventh Bolgarian Conf. on Spectroscopy, Burgas, September, 1976.
[30]A. F. Bunkin, S. G. Ivanov, and N. I. Koroteev, Dokl. Akad. Nauk SSSR **233**, 338 (1977) [Sov. Phys. Dokl. **22**, 338 (1977)].
[31]A. F. Bunkin, S. G. Ivanov, and N. I. Koroteev, Pis'ma Zh. Tekh. Fiz. **3**, 450 (1977) [Sov. Tech. Phys. Lett. **3**, 182 (1977)].
[32]M. D. Levenson, J. J. Song, and G. L. Eesley, Appl. Phys. Lett. **29**, 567 (1976).
[33]S. A. Akhmanov, A. F. Bunkin, S. G. Ivanov, and N. I. Koroteev, Pis'ma Zh. Eksp. Teor. Fiz. **25**, 444 (1977)

[JETP Lett. 25, 416 (1977)].
[34]M. A. Yuratich and D. C. Hanna, a) Opt. Commun 18, 134 (1976); b) Mol. Phys. 33, 671 (1977).
[35]N. I. Koroteev, Paper at Fifth Vavilov Conf. on Nonlinear Optics, Novosibirsk, June, 1977.
[36]I. V. Aleksandrov, Ya. S. Bobovich, N. M. Belyaevskaya, A. V. Bortkevich, and V. G. Maslov, Zh. Eksp. Teor. Fiz. 68, 1274 (1975) [Sov. Phys. JETP 41, 632 (1975)].
[37]M. Born and E. Wolf, Principles of Optics, Pergamon, 1969.
[38]D. S. Belyankin, Kristallooptika (Crystal Optics), Gosgeologizdat, Moscow, 1949.
[39]A. F. Bunkin, S. G. Ivanov, and N. I. Koroteev, in: Teoreticheskaya spektroskopiya (Theoretical Spectroscopy), Nauka, 1977, p. 121.
[40]I. I. Kondilenko, P. A. Korotkov, and V. I. Malyi, Opt. Spektrosk. 36, 486 (1974).
[41]A. F. Bunkin, M. G. Karimov, and N. I. Koroteev, Vestn. Mosk. Univ. Fiz. 19, 1 (1978).
[42]K. W. F. Kohlrausch, Ramanspektren, Akad. Verlag, Leipzig, 1943 (reprint, Edwards Bros.).
[43]W. Proffitt and S. P. S. Porto, J. Opt. Soc. Am. 63, 77 (1973).
[44]Ellipsometry in measurement of surfaces and thin films, Proc. Symposium, ed. E. Passaglia, Washington, 1964.
[45]S. A. Akhmanov, B. V. Zhdanov, A. I. Kovrigin, V. I. Kuznetsov, S. M. Pershin, and A. I. Khlodnykh, Kvantovaya Elektron. (Moscow) 4, 2225 (1977) [Sov. J. Quantum Electron. 7, 1271 (1977)].
[46]C. Flytzanis, in: Treatise in Quantum Electronics, ed. H. Rabin and C. L. Tang, Academic, New York, vol. 1A, 1975, p. III.
[47]P. D. Maker and R. W. Terhune, Phys. Rev. 137, A801 (1965).
[48]N. Bloembergen, Nonlinear Optics, Benjamin, 1963.

Translated by J. G. Adashko

Nonlinear resonances of accelerated atoms and molecules

S. G. Rautian and G. I. Smirnov

Institute of Automation and Electrometry, Siberian Division, USSR Academy of Sciences
(Submitted 16 September 1977)
Zh. Eksp. Teor. Fiz. 74, 1295–1306 (April 1978)

An exact kinetic equation is obtained for the density matrix, suitable for any interaction of a particle with an external field, is obtained. It is used to analyze the singularities of the broadening of various nonlinear resonances under conditions when the excited particles move with constant acceleration over the mean free path in a gas or in a plasma. It is established that resonances of various origins react differently to the accelerated motion of the emitter. Under definite conditions the acceleration can lead to splitting or narrowing of nonlinear spectral structures.

PACS numbers: 32.70.Jz, 33.70.Jg, 41.70.+t

1. INTRODUCTION

In the solution of numerous problems of nonlinear spectroscopy one uses various nonlinear resonances: resonances with saturation of absorption by independent waves, the nonlinear Zeeman effect, and others. Under real conditions active particles are acted upon as a rule by various external forces (the Lorentz force, gravitation, etc.) and the acceleration they produce can alter the shape of the narrow resonances.[1,2] For the indicated effect to be noted, the Doppler frequency shift due to the acceleration **a**,

$$\Delta\omega \sim \mathbf{a}\mathbf{k}\tau \tag{1}$$

(τ is the emission time and **k** is the wave vector) must be comparable with the width of the corresponding nonlinear resonance γ[1]:

$$\Delta\omega \gtrsim \gamma. \tag{2}$$

These situations are encountered in ultrahigh-resolution spectroscopy quite frequently. There is therefore a distinct need for an investigation of the singularities of the broadening under the indicated conditions. This is important in order to obtain exact spectroscopic information on the physical properties in active media, and also for an effective control of the results of the acceleration.

Resonances of various origins react differently to the acceleration of the emitter. In this article we consider the singularities of this transformation for the most promising methods of obtaining ultranarrow nonlinear resonances: a) independent waves interacting with two- and three-level systems, b) the nonlinear Zeeman effect, c) competing resonances in a ring laser.

2. KINETIC EQUATION. GENERAL FORMALISM

In the quantum-mechanical treatment, the energy of the atom (or molecule) is determined by the eigenvalues of the Hamiltonian

$$H = \frac{p^2}{2m} + U(\eta, \xi) + H'(\mathbf{p}, \mathbf{r}; \eta, \xi), \tag{3}$$

where **r** is the coordinate of the mass center, ξ denotes the aggregate of the internal coordinates, and **p** and η are the corresponding momenta:

$$\mathbf{p} = -i\hbar\nabla_{\mathbf{r}}, \quad \eta = -i\hbar\frac{\partial}{\partial\xi}. \tag{4}$$

The first term in (3) takes into account the kinetic energy of the mass center of the atom (whose mass is m); U is the operator of the interaction of the component parts of the atom, and H' describes the action of the external fields and depends on both the translational and the internal coordinates of the atom.

 0038-5646/78/040678-07$02.40